Electronic Structure of Rh_2S_3 and RuS_2, Two Very Active Hydrodesulfurization Catalysts

Agnes Tan‡ and Suzanne Harris*

Department of Chemistry, University of Wyoming, Laramie, Wyoming 82071

Received August 14, 1997

The results of Fenske−Hall band structure calculations for bulk Rh_2S_3 and RuS_2 and for the (210) and (111) surfaces of RuS_2 are described. Although the crystal structures of the two sulfides are quite different, the electronic structure of bulk Rh_2S_3 and RuS_2 share several similarities. Unlike MoS_2, which is also used as a hydrodesulfurization (HDS) catalyst, there is no metal−metal bonding and only negligible metal−sulfur π bonding in both Rh_2S_3 and RuS_2. As a result, both sulfides are characterized by a narrow high energy occupied metal t_{2g} band localized on the metal. Results of calculations for two-dimensional RuS_2 slabs exposing (210) and (111) surface planes provide a description of the electronic structure of 5-, 4-, and 3-coordinate Ru atoms on these surfaces. Stabilization of part or all of the unoccupied Ru e_g band is observed for these surface atoms, and comparisons between the partial densities of states (DOS) of the surface Ru atoms and the orbital structures of isolated coordinatively unsaturated metal centers aid in the interpretation of the surface results. The electronic environments of the surface Ru atoms are also compared to the electronic environments and reactivities of metal centers found in d^6 transition metal complexes that incorporate thiophenic ligands. These comparisons suggest that if the heterogeneous and homogeneous HDS mechanisms are related, then 3-coordinate surface Ru atoms such as those found on the (111) surface could provide active sites.

Introduction

We recently reported the application of a new Fenske−Hall tight-binding band structure method to the bulk and surface electronic structure of MoS_2.[1] We are interested in the surface chemistry of inorganic solids which serve as catalysts in heterogeneous processes, and this computational approach provides a new tool to study these materials. In the hydrodesulfurization (HDS) process a transition metal sulfide based catalyst is used to remove sulfur from aromatic molecules such as thiophene, and we are particularly interested in understanding how the electronic structures of transition metal sulfides are related to their activity as HDS catalysts. Two sulfides that exhibit particularly high HDS activity are Rh_2S_3 and RuS_2,[2] and results of Fenske−Hall band structure calculations for these two materials are described in this paper.

The first section of the paper describes the calculational details. This is followed by a discussion of the calculated electronic structures of bulk Rh_2S_3 and RuS_2. Although Rh_2S_3 is known to exhibit very high HDS activity, little is known about its electronic structure or the surfaces which provide the active site for HDS reactions. Our results for Rh_2S_3 provide the first description of the electronic structure of this sulfide. RuS_2 has been the subject of earlier ab initio calculations,[3,4] and we compare our results to previous theoretical and experimental descriptions of its electronic structure. These results for bulk RuS_2 provide the basis for studies of the electronic structure of particular surfaces that may provide active sites for HDS catalysis, and the next section of the paper describes the calculated electronic structure of the (210) and (100) surfaces of RuS_2. Since binding and activation of thiophenic molecules on an active HDS catalyst are believed to occur at coordinatively unsaturated metal centers, we consider the electronic properties of such sites on the RuS_2 surfaces. Finally, we consider how a thiophenic molecule might bind and/or react at these coordinatively unsaturated Ru sites. As part of our study of HDS catalysis we have also investigated the relation between bonding and reactivity in transition metal complexes which serve as homogeneous models for the heterogeneous HDS process,[5,6] and we compare the metal centers in these complexes to the metal sites on RuS_2.

Table 1. Irreducible Brillouin Zones (IBZ) and Number of *k* Points

	IBZ	no. of *k* points
solids		
RuS_2	$Pm\bar{3}$	176
Rh_2S_3	Pmmm	125
surfaces		
RuS_2 (210)	rectangular	100
RuS_2 (111)	2-D hexagonal	91

Calculational Details

All calculations were carried out using the Fenske−Hall band structure program described in a recent report.[1] Calculations on Rh_2S_3 and RuS_2 are based on the known crystal structures of these solids.[7,8] Surface calculations for RuS_2 assumed unreconstructed surfaces. The *k* points were sampled from the irreducible Brillouin zone (IBZ) of the appropriate Patterson space groups, as documented by Ramírez and Böhm;[9,10] these are listed in Table 1.

‡ Present Address: Institute of Molecular and Cell Biology, National University of Singapore, Kent Ridge, Singapore 119260.

(1) Tan, A.; Harris, S. *Inorg. Chem.,* 2205.
(2) Pecoraro, T. A.; Chianelli, R. R. *J. Catal.* **1981,** *67,* 430.
(3) Holzwarth, N. A. W.; Harris, S.; Liang, K. S. *Phys. Rev. B* **1985,** *32,* 3745.
(4) Fréchard, F.; Sautet, P. *Surf. Sci.* **1995,** *336,* 149.
(5) Harris, S. *Organometallics* **1994**, *13,* 2628.
(6) Palmer, M.; Carter, K.; Harris, S. *Organometallics* **1997**, *16,* 2448.
(7) Parthé, E.; Hohnke, D.; Hulliger, F. *Acta Crystallogr.* **1967,** *23*, 832.
(8) Sutarno; Knop, O.; Reid, K. I. G. *Can. J. Chem.* **1967**, *45,* 1391.
(9) Ramírez, R.; Böhm, M. C. *Int. J. Quantum Chem.* **1986,** *30,* 391.

S0020-1669(97)01028-8 CCC: $15.00
Published on Web 04/08/1998

Atomic basis functions were obtained by fitting the results of Xα (Herman−Skillman) calculations[11] for a given atomic charge to Slater type orbitals (STO's).[12] The Ru and Rh 4d and S 2p functions were were fit to double-ζ STO's; all other functions were fit to single-ζ STO's. As discussed previously,[1] transition metal basis functions for molecular Fenske−Hall calculations are generally chosen by calculating a modified Mulliken charge for the metal which is based on the valence d orbital populations only; this modified charge, rounded to the nearest integer, determines the choice of the 1s through valence d orbital functions. This procedure for selecting basis functions for transition metals is unsuitable for the band structure calculations, since the valence *d* functions obtained are too diffuse and lead to bandwidths that are too wide. This is particularly true for second (and third) row transition metals, where the basis functions need to be more contracted; this is less the case for the smaller first row transition metals. The problem of wide bandwidths is most acute for compounds with the pyrite structure (RuS_2, FeS_2, NiS_2, CoS_2), and metal basis functions used to study these compounds (especially for Ru) must be significantly more contracted (see Discussion below). Therefore the 1s through valence d orbital basis functions used for Ru in the calculations for RuS_2 were chosen by fitting the width of the d band to the width obtained from ab initio calculations on RuS_2; since such calculations are unavailable for Rh_2S_3, the Rh functions were chosen by extrapolating from calculations on other transition metal sulfides.

The results reported here for Rh_2S_3 used 1s through 4d atomic basis functions corresponding to $Rh^{+2.5}$. As in molecular calculations, the Ru and Rh 5s and 5p functions were both chosen to have exponents of 2.2. Sulfur basis functions corresponding to *S*(0) were used for calculations on Rh_2S_3, where the sulfur atoms have a formal 2− oxidation state, and *S*(+0.5) for RuS_2 where the sulfur atoms are found in disulfide units (S_2^{2-}) and thus have a formal oxidation state of 1−. The highly contracted Ru (+3.2) basis functions used in the calculations were chosen to match the combined bandwidth of the t_{2g} and e_g bands resulting from an ab initio density functional calculation.[3] These earlier results were shown to be in close agreement with experiment. The use of *S*(+0.5) functions reproduces the experimental p bandwidth of RuS_2. Although the experimental widths of the metal and sulfur bands are reproduced by this choice of basis functions, the metal levels are significantly destabilized with respect to the S p band, resulting in a ∼4 eV gap between the sulfur p and Ru t_{2g} bands; this gap is not observed in the experimental photoelectron spectrum.[3] As discussed previously we have found such a gap (of varying width) to be present in all our calculations on second row transition metal sulfides, and we attribute the gap to approximations used in the Fenske−Hall method.[1] The gap calculated for RuS_2 is particularly large, and it appears that the point charge approximation in combination with the RuS_2 structure (where both the first and second sets of nearest neighbors of each Ru atom carry a negative charge) is responsible for the calculated gap. The Ru 4d levels could be stabilized somewhat through the use of more diffuse functions, but this would result in an increase in the overall width of the occupied bands. Thus we have chosen not to use more diffuse basis functions.

Results and Discussion

Electronic Structure of Bulk Rh_2S_3. The crystal structure of Rh_2S_3 is unique and is known as the "Rh_2S_3" structure (Figure 1a). Each Rh^{3+} center in the crystal is approximately octahedrally coordinated by six sulfurs, and the structure is characterized by face-sharing pairs of distorted [RhS_6] octahedra. These octahedral pairs form two-dimensional sheets through shared S^{2-} ions. Although these sheets are also linked in the third dimension through further sharing of S^{2-} ions (this leads to a distorted tetrahedral arrangement around each S^{2-} ion), it is useful to envision the sheets of octahedral pairs as being arranged in layers which show the stacking sequence *ABABAB*.... The structure of an isolated face sharing octahedral pair and the arrangement of two layers of these octahedral pairs are shown in Figure 1a.

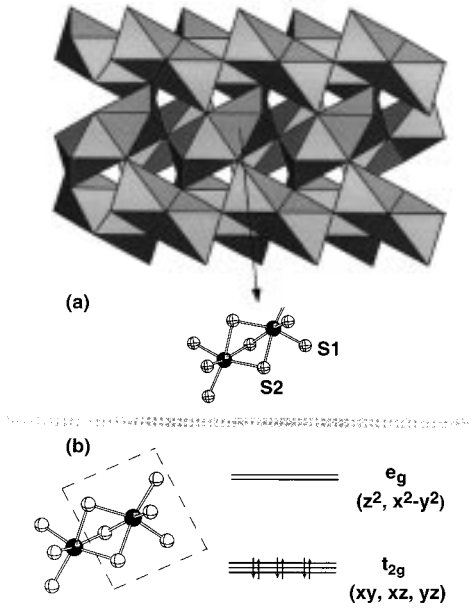

Figure 1. (a) Structure of Rh_2S_3. The polyhedral representation illustrates two layers of face-sharing octahedral [RhS_6] units connected through tetrahedral S atoms. One of the face-sharing units is illustrated in ball-and-stick representation; (b) Crystal field splitting of the Rh 4d orbitals resulting from the local octahedral environment.

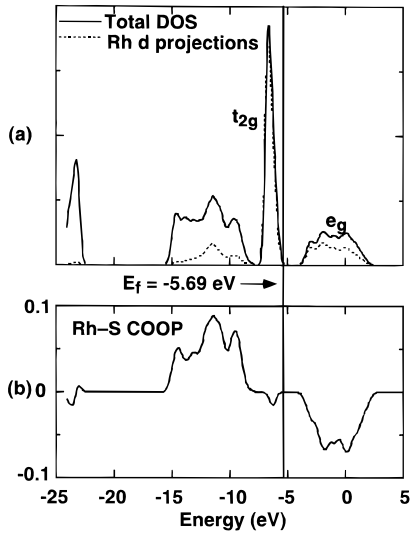

Figure 2. (a) Total and Rh 4d partial densities of states (DOS) curves for Rh_2S_3; (b) crystal orbital overlap projection (COOP) of all the RhS bonds in one [RhS_6] octahedron.

Since each Rh^{3+} d^6 center lies within an approximate octahedron of sulfurs, the local crystal field should split the metal 4d orbitals into t_{2g} and e_g sets (Figure 1b), with the e_g orbitals unoccupied. This splitting is apparent in the calculated density of states (DOS) of Rh_2S_3 (Figure 2a), where the occupied Rh t_{2g} band is separated by a semiconducting gap from the vacant e_g band. The semiconducting gap is calculated to be 2.0 eV. The crystal orbital overlap projection (COOP) of all the Rh−S bonds in one RhS_6 octahedron, Figure 2b, also displays the expected features: the sulfur band is Rh−S bonding, while the Rh band, especially the e_g component, is antibonding. The t_{2g} band is almost entirely Rh in character,

(10) Ramírez, R.; Böhm, M. C. *Int. J. Quantum Chem.* **1988,** *34*, 571.
(11) Herman, F.; Skillman, S. *Atomic Structure Calculations;* Prentice Hall: Englewood Cliffs, NJ, 1963.
(12) Bursten, B. E.; Jensen, R. J.; Fenske, R. F. *J. Chem. Phys.* **1978,** *68*, 3320.

Table 2. Calculated Mulliken Charges (q_A), Energy Levels ($F_{aa}°$, EV, for Metal d and Sulfur p Orbitals), and Potential Energies ($-Q_A$, eV) for Bulk RuS_2 and Rh_2S_3

		q_A	$F_{aa}°$	$-Q_A$
RuS_2	Ru	0.96	−2.28	−9.21
	S	−0.48	−9.44	4.79
Rh_2S_3	Rh	+0.79	−6.80	−7.80
	S1	−0.49	−11.13	5.24
	S2	−0.54	−10.88	5.67

indicating that there is little π bonding between the Rh and S atoms. This is consistent with the tetrahedral geometry of the S atoms and the fact that all of the S valence electrons are utilized in the formation of Rh−S σ bonds.

An examination of the crystal structure of Rh_2S_3 reveals that the octahedral environment of each Rh atom is severely distorted. This distortion can be traced to the electronic environment of the Rh atoms. In an undistorted octahedral geometry the two d^6 Rh atoms in each pair of face sharing octahedra would be within bonding distance. This would lead to strong interactions between the filled t_{2g} sets of orbitals on the two metals and a strong net antibonding interaction between the two metal centers. The Rh centers therefore move apart in order to minimize these antibonding interactions. This results in the observed distorted octahedral coordination geometries, nonbonding Rh−Rh distances, and (since at the longer Rh−Rh distance the bands having Rh−Rh bonding and antibonding character collapse into a group of relatively flat bands) the relatively narrow t_{2g} band observed in the density of states.

Further examination of the crystal structure of Rh_2S_3 shows that, although all of the Rh atoms are equivalent, two types of sulfur atoms can be distinguished. This inequivalence is reflected in the calculated Mulliken charges and diagonal elements of the Hartree−Fock matrix listed in Table 2. If one considers a "layer" of octahedron pairs, the less negatively charged sulfur atoms, S1 in Figure 1a, may be identified as those occupying the corners of two pairs, while the more negative sulfur atoms, S2, occupy a corner of one pair and an edge of another. This is consistent with the fact that the Rh−S bonds associated with the corner atoms are shorter on average, indicating a greater covalency.

Unfortunately, no experimental measurements of the semiconducting gap or the photoelectron spectrum of Rh_2S_3 have been reported; this means that no data is available with which to compare either the band gap or the features of the DOS curve. The calculated DOS curve exhibits a slight separation between the top of the sulfur bands and the bottom of the metal 4d valence band. Our previous results for MoS_2 and the results discussed below for RuS_2 suggest that the actual separation may be smaller or non existent. As mentioned above, although Rh_2S_3 is one of the most active HDS catalysts, little is known about its properties. Our results provide a clearer picture of the bulk electronic structure of this material, but further experimental characterization (particularly of the prominent surfaces) is also needed.

Electronic Structure of Bulk RuS_2. While each Ru^{2+} center in RuS_2 is also approximately octahedrally coordinated by six sulfurs, the structures of RuS_2 and Rh_2S_3 are very different. As illustrated in Figure 3a, RuS_2 exhibits the pyrite structure (a NaCl structure in which the anions have been replaced by S_2^{2-} ions), where the octahedral Ru^{2+} ions are linked via S_2^{2-} ions in a three-dimensional network. In this environment we also expect to observe a splitting of the Ru d orbitals into t_{2g} and e_g sets (Figure 3b). Since Ru^{2+} is a d^6 ion, the t_{2g} orbitals should be filled while the e_g orbitals remain empty. This splitting is

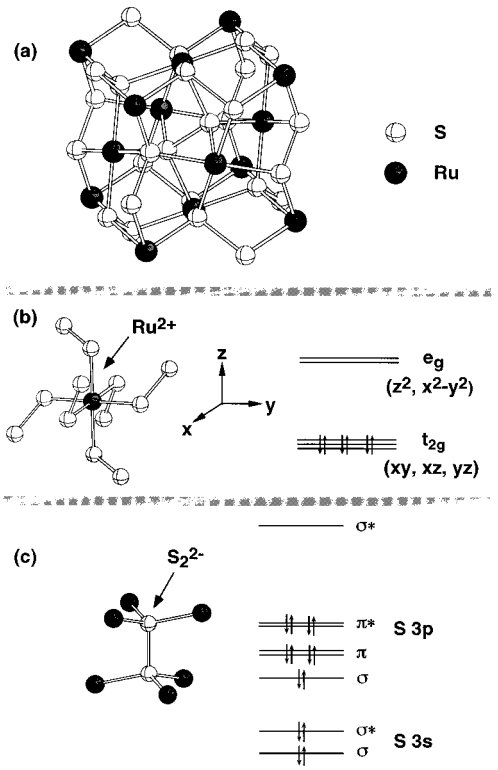

Figure 3. (a) Illustration of a portion of the pyrite structure of RuS_2; (b) local coordination environment of a Ru^{2+} center and the crystal field splitting of the Ru 4d orbitals resulting from this environment; (c) local environment and orbital structure of a disulfide (S_2^{2-}) ion.

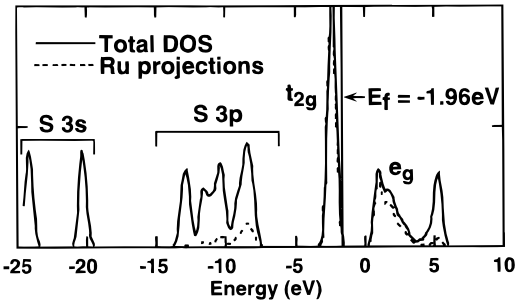

Figure 4. Total and Ru 4d partial DOS curves for bulk RuS_2.

observed in the calculated (DOS) plot for RuS_2 (Figure 4) where the Fermi level lies at the top of the filled t_{2g} band and the energy difference between the top of the t_{2g} band and the bottom of the empty e_g band constitutes the semiconducting gap. The lower energy sulfur bands reflect the bonding within the S_2^{2-} units (Figure 3c). The lowest energy bands correspond to the S_2^{2-} 3s σ and σ* orbitals, while the structure in the sulfur *p* band arises from the S_2^{2-} 3p σ, π, and π* orbitals.

The electronic structure of RuS_2 has been the subject of both a density functional calculation[3] and a rigorous Hartree−Fock (HF) calculation.[4] The DOS obtained from the density functional calculation of Holzwarth et al. was shown to be in close agreement with the experimental photoelectron spectrum of RuS_2. Comparison of our calculated DOS with the experimental photoelectron spectrum of RuS_2 reported by Holzwarth et al.[3] shows that while the general features of the DOS are described well by our results, the calculated ~4 eV gap between the sulfur *p* and Ru t_{2g} bands is not observed in the experimental photoelectron spectrum. In addition, the splitting between the sulfur s and p bands is somewhat larger than the splitting observed in the photoelectron spectrum. As a result, the total

width of the occupied bands is about 6 eV wider than is experimentally observed. The calculated ($t_{2g} - e_g$) band gap of about 2.5 eV is also significantly larger than the experimental value of 1.3 eV.[13]

The results of the recent HF calculation for RuS_2 do not appear to represent the electronic structure of RuS_2 as well as the results of Holzwarth's density functional calculation.[4] Although the calculated DOS does not exhibit a gap between the occupied sulfur p and metal d bands, the total width of the occupied bands is also calculated to be about 6 eV too wide, and the ligand field splitting is so wide that it is not even reported. It should be noted, however, that it is generally recognized that Hartree−Fock band structure calculations overestimate band gaps (e.g. rigorous HF calculations on TiO_2, ZrO_2, and V_2O_5,[14−16] all of which contain d^0 metals, yielded a gap between the occupied oxygen *p* band and the unoccupied metal d band about 3−4 times larger than the experimental value). Another noticeable feature of the HF results for RuS_2 is a relatively large sulfur contribution to the high energy occupied t_{2g} bands. This suggests a greater π covalency of the Ru−S bonds than is probably correct and contradicts the experimental results and the results of both Holzwarth's and our calculations. Our results, on the other hand, may slightly underestimate the π contribution to the Ru−S bonds.

It interesting to note that the only nonempirical calculations of the band structures of pyrites which yield DOS curves in close agreement with experiment[3,17,18] all invoke some form of density functional theory to calculate exchange and correlation corrections. The reason for this is not clear. While our calculations do not reproduce the detailed features of Holzwarth's calculated DOS for RuS_2, they do model the qualitative aspects of the band structure of RuS_2 quite well and therefore provide a basis for the study of RuS_2 surfaces.

Surfaces. Rh_2S_3 and RuS_2, two of the most active HDS catalysts, exhibit approximately the same catalytic activity as the Co- or Ni-promoted MoS_2 used in many industrial HDS processes. Although the crystal structures, and thus the surface structures, of Rh_2S_3, RuS_2, and promoted MoS_2 are clearly very different, their similar HDS activities suggest that similar active sites may be found on the active surfaces of the sulfides. While it is generally accepted that active sites involve coordinatively unsaturated metal centers, there is little agreement as to exactly which metal site is active or how many sulfur vacancies exist in the metal coordination sphere at this active site. To try to understand the similarities and differences in coordinatively unsaturated metal centers on the surfaces of materials such as MoS_2, Co- or Ni-promoted MoS_2, Rh_2S_3, and RuS_2, we have begun a systematic study of the electronic structure of possible active surfaces on these sulfides. We recently reported our initial results for MoS_2, and we have also begun studies related to the Co/Mo/S- and Ni/Mo/S-promoted phases of MoS_2.[19] We report here our first results for surfaces of RuS_2. While the electronic structures of surfaces of both Rh_2S_3 and RuS_2 are of interest, we have chosen to consider RuS_2 first, because crystals of RuS_2 have been studied much more thoroughly than those of Rh_2S_3, and possible active surfaces have been proposed.[20] It is still not known with certainty, however, which particular surfaces provide the HDS activity.

Two surfaces, (100) and (111), of RuS_2 have been the subject of recent Hartree−Fock band structure calculations.[4] Our studies consider a different surface, (210), and a different termination of the (111) surface and focus on coordinatively unsaturated Ru sites on these surfaces. The (210) and (111) surfaces were chosen for two reasons: first, it has been observed that (210) faces predominate on the surfaces of larger crystals of RuS_2, while smaller crystals preferentially show (111) faces,[20] and second, these surfaces allow us to study different types of coordinatively unsaturated Ru centers.

To study the electronic structures of surfaces it is necessary to carry out calculations on two-dimensional slabs of finite thickness. One or both of the surfaces of the slab then represents a surface of interest. The slabs utilized for the RuS_2 calculations incorporated three or four layers of metal centers and their surrounding ligands and were constructed such that both the stoichiometry of the slab and the integrity of the disulfide units were preserved. This provides a reasonable representation of the "bulk" as well as surface atoms and also limits the size of the unit cell.

RuS_2 (210) and (111) Surfaces. The structures of portions of the slabs used to represent the (210) and (111) surfaces are shown in Figure 5. A side view of a portion of the (210) slab is shown in Figure 5a (the slab repeats in both horizontal directions); the slightly tilted view in Figure 5b provides a view of the structure of the (210) surface. Both surfaces of this slab are identical. The (210) surface exposes both 4- and 5-coordinate Ru atoms. The exposed S_2 units have either one or two bonds missing; in the first case (labeled S^a in Figure 5b), a 3-coordinate S atom is bound to a 4-coordinate S atom and two Ru atoms, while in the second case (labeled S^b in Figure 5b) each S atom of the S_2 unit is missing one bond. These two S^b atoms are not entirely equivalent, however, since one S atom is attached to a 4-coordinate and a 6-coordinate Ru atom while the other is attached to a 4-coordinate and a 5-coordinate Ru atom. This surface is not flat but is instead characterized by troughs lined by both 4- and 5-coordinate Ru centers.

A portion of the (111) slab is illustrated in Figure 5c and 5d. This slab was constructed so that one surface exposes only 3-coordinate Ru atoms and the other only S_2 units. All the surface S_2 units have three missing bonds; on one type of S_2 unit (labeled S_2 in Figure 5c) this unsaturation is concentrated on one atom, while the other type of S_2 units (labeled S_2' in Figure 5c) have one 2-coordinate and one 3-coordinate atom. Due to the complexity of the structure, all of the bonds involving these sulfur atoms are not shown in Figure 5c. While the Ru atoms define a flat surface, it should be noted that there are actually four *orientationally* inequivalent Ru centers on this surface. They are inequivalent because the plane of the three sulfur atoms in the coordination sphere of the respective metal atoms are oriented differently with respect to the surface; only one of them is approximately parallel to the surface.

The total DOS curves for bulk RuS_2, the (210) slab, and the (111) slab are shown in Figure 6. Projections of the Ru orbitals in bulk RuS_2, the 5- and 4-coordinate Ru orbitals on the (210) surface, and the 3-coordinate Ru orbitals on the (111) surface are also shown in Figure 6a−d, respectively. Comparisons of the total and projected DOS curves show that the breaking of bonds and concomitant loss of Ru−S σ-antibonding interactions

(13) Bichsel, R.; Levy, F.; Berger, H. *J. Phys. C* **1984,** *17*, L19.
(14) Fahmi, A.; Minot, C.; Silvi, B.; Causá, M. *Phys. Rev. B* **1993,** *47*, 11717.
(15) Orlando, R.; Pisani, C.; Roetti, C.; Stefanovich, E. *Phys. Rev. B* **1992,** *45*, 592.
(16) Kempf, J. Y.; Silvi, B.; Dietrich, A.; Catlow, C. R. A.; Maigret, B. *Chem. Mater.* **1993**, *5*, 641.
(17) Bullett, D. W. *Solid State Phys.* **1982,** *15*, 6163.
(18) Temmerman, W. M.; Durham, P. J.; Vaughan, D. J. *Phys. Chem. Minerals* **1993,** *20*, 248.
(19) Tan, A.; Harris, S. In preparation.
(20) Reyes, J. A. D. L.; Vrinat, M.; Geantet, C.; Breysse, M. *Catalysis Today* **1991,** *10*, 645.

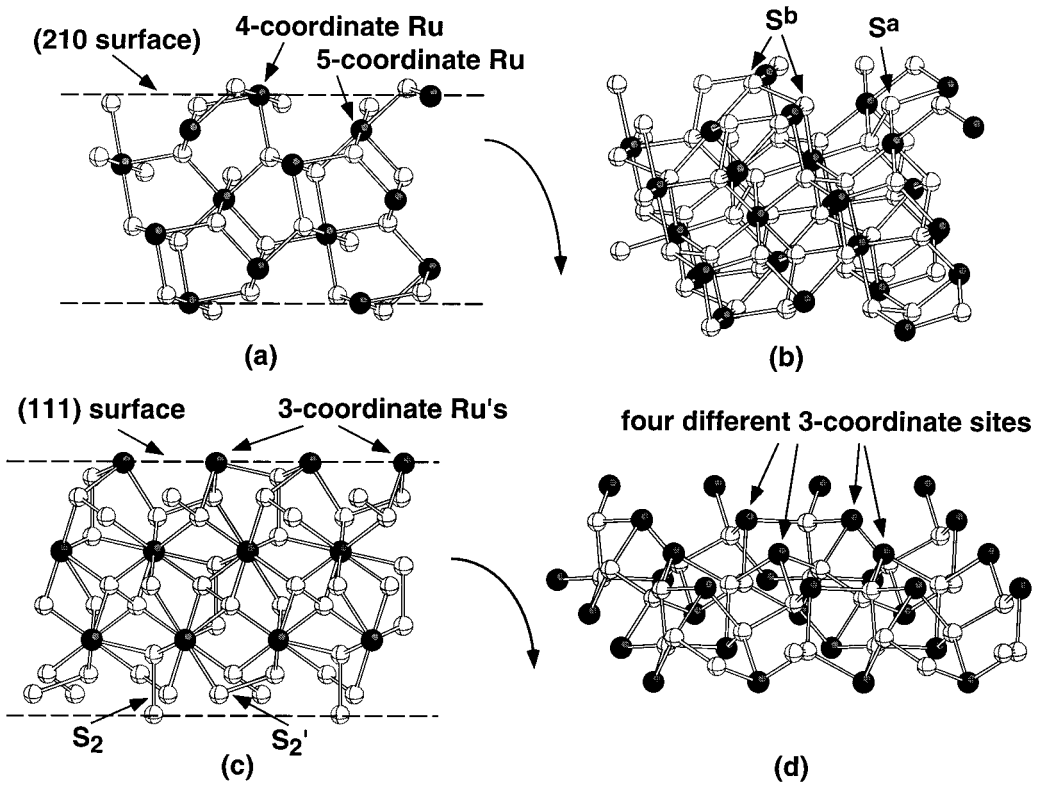

Figure 5. Illustrations of portions of the slabs used to study the (210) and (111) surfaces of RuS_2. (a, b) Side and slightly tilted views of a portion of the (210) slab; (c, d) side and slightly tilted views of a portion of the (111) slab. The bottom layer of S_2 units has been omitted in (d) in order to simplify the diagram. The labels on various S atoms are discussed in the text.

results in the lowering in energy of part or all of the e_g band associated with the surface Ru atoms. Since this band is Ru−S antibonding, the magnitude of this stabilization increases as the degree of coordinative unsaturation increases. Thus the order of stabilization is (210) 5-coordinate < (210) 4-coordinate < (111) 3-coordinate. This stabilization is so large on the Ru-rich (111) surface that part of the e_g band lies below the Fermi level and the surface is found to be metallic.

A better understanding of the nature of the stabilized bands can be obtained by comparing the expected metal orbital structure for isolated 5-, 4-, and 3-coordinate metal atoms with the projected partial densities of states for the 5-, 4-, and 3-coordinate Ru surface atoms, respectively. These are shown in Figures 7−9. The qualitative orbital diagram shown on the left of Figure 7 illustrates the effects of removing one ligand from an octahedral metal center to form a square pyramidal 5-coordinate metal center. If the bond is broken along the *z* axis, the major orbital stabilization occurs for the d_{z^2} orbital. The $d_{x^2-y^2}$ orbital remains high in energy, while the three lower energy t_{2g} orbitals remain nearly degenerate (particularly when there is little π interaction between the metal and ligands). The projections of the 5-coordinate Ru (210) surface d orbitals show these same effects. The unoccupied e_g band of RuS_2 is split into two components, and the projection of the d_{z^2} orbital makes it possible to clearly identify the stabilized d_{z^2} band. The other two orbital projections show the combined DOS for the $d_{x^2-y^2}$ and d_{xy} orbitals and for the d_{xz} and d_{yz} orbitals. It is necessary to project these orbitals out in pairs because although we can control the orientation of the *z* axis, and thus the orientation of the *xy* plane, of the local coordinate system of the Ru atoms in the band structure calculations, we cannot control the exact orientation of the individual *x* and *y* axes. This means that metal bands which correspond, for example, to either the $d_{x^2-y^2}$ or d_{xy} orbitals on the left side of the diagram must be described in the results of the band structure calculations as mixtures of $d_{x^2-y^2}$ and d_{xy} orbitals and must be projected out together. Thus in the combined projection of the $d_{x^2-y^2}$ and d_{xy} orbitals, the lower energy part of the projection corresponds to the d_{xy} component of the occupied t_{2g} band, while the higher energy projection corresponds to the unoccupied $d_{x^2-y^2}$ band. Although the Ru d_{xz} and d_{yz} orbitals must also be projected out together, these two orbitals contribute only to the occupied t_{2g} band and project out together in the same energy range.

The effects of breaking two bonds to form a 4-coordinate metal center are illustrated on the left of Figure 8. In this case both e_g orbitals are stabilized, but the orbital which points directly at the ligand vacancies (d_{yz} in the coordinate system shown in Figure 8) is stabilized more. Once again the three lower energy t_{2g} orbitals are expected to remain nearly degenerate. The loss of two ligands also stabilizes a high-energy sp hybrid orbital. All of these features can be seen in the Ru DOS curves for the 4-coordinate Ru centers on the RuS_2 (210) surface. The high-energy unoccupied band centered at ∼8 eV corresponds to the high-energy metal face-sharing hybrid shown at the left. Although it is necessary, as discussed above, to project out the $d_{x^2-y^2}$ and d_{xy} orbitals and the d_{xz} and d_{yz} orbitals in pairs, we can readily relate the Ru d bands to the orbitals of an isolated 4-coordinate metal center. The lower energy components of the $d_{x^2-y^2}$, d_{xy} and the d_{xz}, d_{yz} projections and the major component of the d_{z^2} band together make up the occupied t_{2g} band; this corresponds to the three t_{2g} orbitals shown on the left. The higher energy unoccupied components of the d_{xz}, d_{yz} and $d_{x^2-y^2}$, d_{xy} projections make up the "e_g" band and correspond to the d_{yz} and $d_{x^2-y^2}$ orbitals, respectively, shown on the left. The small contribution of the d_{z^2} orbital to the higher energy $d_{x^2-y^2}$ band can be attributed to the local C_{2v} symmetry of the 4-coordinate Ru center which allows mixing of the two orbitals.

The presence of both 5- and 4-coordinate Ru centers on the

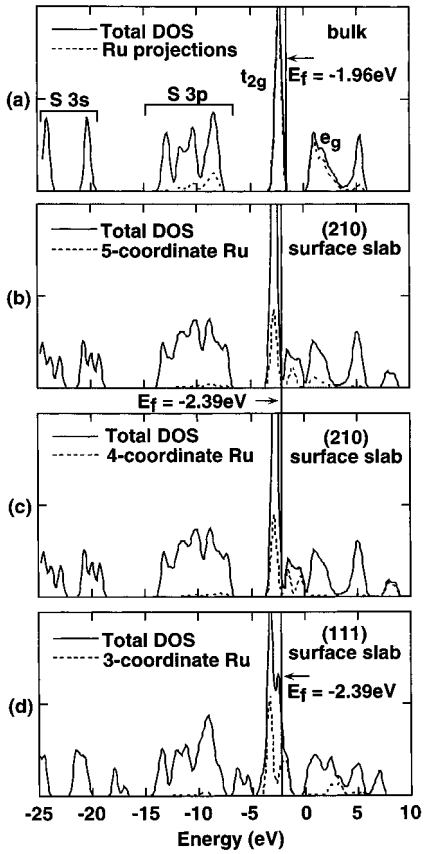

Figure 6. Comparison of total DOS curves for (a) bulk RuS_2, (b, c) the (210) surface slab, and (d) the (111) surface slab. The partial DOS curves for the 4d orbitals of 5-, 4-, and 3-coordinate surface Ru atoms are also shown in (b), (c), and (d), respectively.

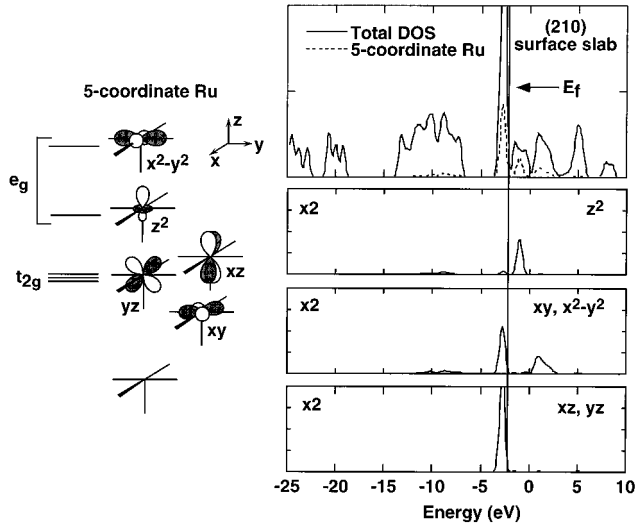

Figure 7. Comparison of the orbital structure of an isolated square pyramidal 5-coordinate metal center with the projections of the 5-coordinate surface Ru orbitals on the RuS_2 (210) surface. The scale of the plots for the orbital projections is two times larger than the scale for the total DOS; this is indicated on each plot by "×2".

(210) surface of RuS_2 thus introduces three new bands into the semiconducting gap of bulk RuS_2. Two of these bands arise from the 4-coordinate Ru center and the other from the 5-coordinate Ru center. Neither of these newly stabilized bands is occupied in the stoichiometric slab studied here, and this is reflected in the calculated charges for the surface Ru atoms (Table 3), which differ little from the charges of the "bulk" Ru

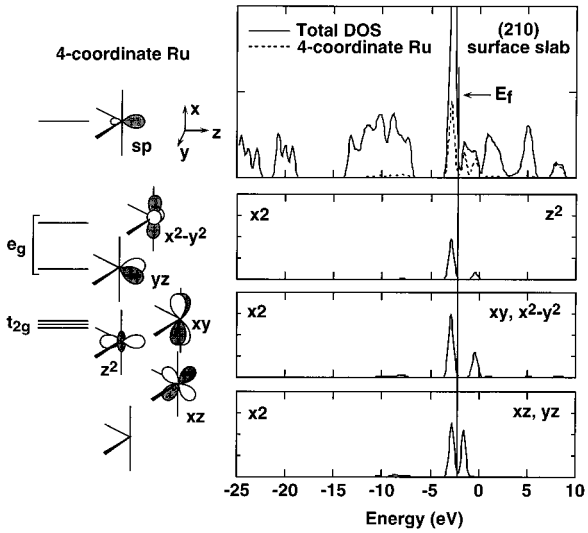

Figure 8. Comparison of the orbital structure of an isolated 4-coordinate metal center with the projections of the 4-coordinate surface Ru orbitals on the RuS_2 (210) surface.

Table 3. Calculated Mulliken Charges[a] of Atoms in the RuS_2 (210) and (111) Slabs

	atom	charge
bulk RuS_2	Ru	+0.96
	S	−0.48
(210) slab	4-coord Ru	+0.95
	5-coord Ru	+0.96
	"Bulk" Ru	+0.97
	3-coord S[a]	−0.48
	3-coord S[b]	−0.53
	"bulk" S	−0.44
(111) slab	3-coord Ru	+0.91
	"bulk" Ru	+0.99
	1-coord S	−0.72
	2-coord S	−0.57
	3-coord S	−0.50
	"bulk" S	−0.45

[a] Values for surface S atoms are averaged over similar atoms. Actual differences between the values for these slightly inequivalent atoms are negligible (<0.01*e*). Superscript a and b refer to atoms as labeled in Figure 5b.

atoms in the slab or the Ru atoms in bulk RuS_2. The energies of the new bands do suggest, however, that reduction of this surface should have a greater effect on the 4-coordinate Ru center, since the lowest energy band above the Fermi level is associated with the 4-coordinate Ru center. The sulfur atoms on this surface, though not all equivalent, are similar in that each sulfur is missing only one bond. While the broadening of the lower energy occupied bands reflects the presence of several different types of sulfur atoms in the slab, the surface sulfur atoms are only slightly reduced compared to the sulfur atoms in bulk RuS_2.

The effects of breaking three metal−ligand bonds to form a pyramidal 3-coordinate metal center are illustrated on the left of Figure 9. In this case both of the e_g orbitals are stabilized but remain degenerate, while the t_{2g} orbitals show little change in energy. The loss of three ligands also introduces a new stabilized sp hybrid orbital at an energy even lower than that observed for the 4-coordinate metal center. These features are also apparent in the Ru DOS curves for the 3-coordinate Ru centers on the RuS_2 (111) surface. The sp hybrid corresponds to the unoccupied Ru band centered at ∼3 eV. Once again only the Ru d_{z^2} band projects out cleanly, but the bands can still be related to the orbitals of the isolated 3-coordinate center

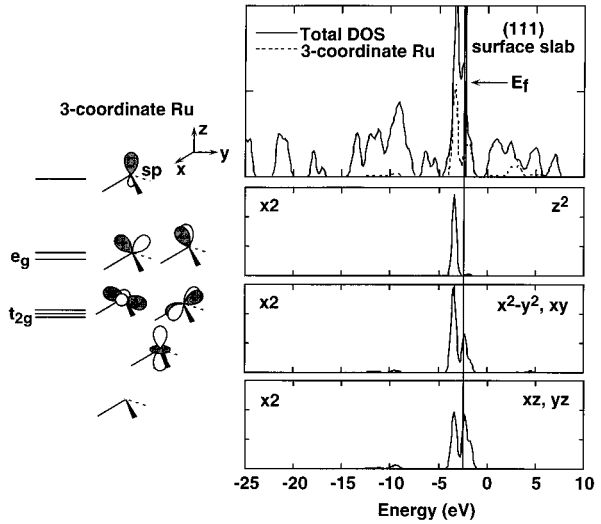

Figure 9. Comparison of the orbital structure of an isolated pyramidal 3-coordinate metal center with the projections of the 3-coordinate surface Ru orbitals on the RuS_2 (111) surface.

shown on the left of the figure. The d_{z^2} band and lower energy components of both the d_{xz}, d_{yz} and $d_{x^2-y^2}$, d_{xy} bands correspond to the three occupied t_{2g} orbitals on the left and thus make up the occupied t_{2g} band of the surface Ru atoms. The higher energy components of the d_{xz}, d_{yz} and $d_{x^2-y^2}$, d_{xy} bands correspond to the two e_g orbitals shown on the left and thus make up the e_g band of the surface Ru atoms. The e_g band is now stabilized to such a great extent that it is actually partially occupied. The calculated charges listed in Table 3 show that even for this stoichiometric slab the surface Ru atoms are slightly reduced relative to the Ru atoms in bulk RuS_2 and the "bulk" Ru atoms in the slab.

The total DOS curve for the (111) surface slab also shows two new occupied bands centered at approximately −17 and −6 eV. These arise from the destabilized sulfur s and p orbitals of the highly coordinatively unsaturated sulfur atoms on the "back" of the slab. These sulfur atoms, which are bound to only one other sulfur atom, are significantly reduced relative to both the bulk and other coordinatively unsaturated sulfur atoms. Bearing in mind the artificial 4 eV energy separation between the sulfur *p* and Ru t_{2g} band in the bulk calculation, it is likely that the top of this *p* band may actually be pushed to or above the Fermi level. In the latter case, the sulfur *p* band would be partially depopulated, resulting in a lower negative charge.

Thiophene Binding and Activation on RuS_2: Comparisons with Molecular Systems. It is unlikely that unrelaxed surfaces composed entirely of coordinatively unsaturated Ru and S atoms are the actual surfaces found under hydrotreating conditions. At the same time, however, the full (210) and (111) surfaces allow us to compare the electronic structures of several types of coordinatively unsaturated Ru sites and to consider how a thiophenic molecule might bind to each of these sites. Several molecular complexes that incorporate thiophenic molecules bound to metal centers having the same coordination geometry and orbital configuration observed for the Ru centers on the (210) and (111) surfaces of RuS_2 have been synthesized and characterized. Examples of relevant complexes are illustrated in Chart 1. In $[(CO)(Ph_3P)CpRu(2\text{-}Me(SC_4H_3))]^+$ (**1**), thiophene binds through the sulfur atom to a 5-coordinate Ru(II) d^6 center.[21] Since the orbital structures of the Ru center in **1** and

Chart 1

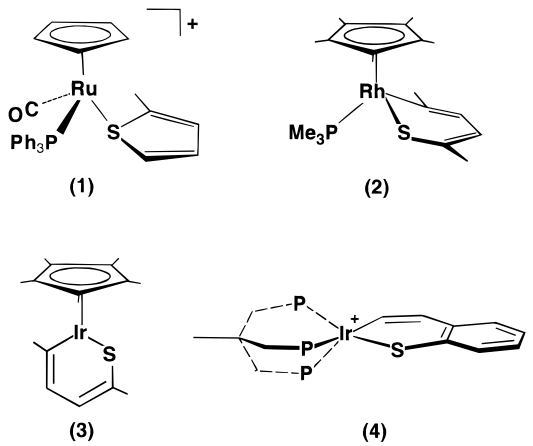

of other d^6 metals in similar complexes[22] resemble that of the 5-coordinate Ru center on the (210) RuS_2 surface, a thiophenic ligand should also be able to bind through the sulfur atom to such a surface site. None of the six-coordinate $M(d^6)-\eta^1$-S-bound complexes exhibits reactivity leading to C−S bond cleavage or desulfurization of the thiophene ring, however, suggesting that while thiophene might bind to the 5-coordinate surface site it is unlikely that this binding would be a precursor to desulfurization.

The syntheses, structures, and reactivities of complexes such as $Cp^*(PMe_3)Rh[C,S\text{-}2,5\text{-}Me_2(SC_4H_2)]$ (**2**),[23] $Cp^*Ir[C,S\text{-}2,5\text{-}Me_2(SC_4H_2)]$ (**3**),[24] and $[(triphos)Ir(C,S(SC_8H_6)\,]^+$ (**4**)[25] suggest that the 4-coordinate Ru center on the (210) surface or the 3-coordinate Ru center on the (111) surface is a better candidate for a possible active site. Complexes **2**, **3**, and **4** are all believed to form via initial η^1-S binding of a thiophenic molecule to a reduced metal center; metal insertion into the ring is then accompanied by an oxidative addition or formal transfer of electrons from the metal to the thiophenic ligand. In addition, Bianchini has shown that in complexes such as **4**, desulfurization of the thiophenic ring can be achieved by sequential H^-/H^+ addition.[26] Desulfurization of the thiophenic ligand in these metal-inserted complexes appears to require a coordination vacancy since desulfurization has not been achieved in 6-coordinate complexes such as **2**. Under the reducing atmosphere of the high H_2 pressures used in HDS, the active surface of RuS_2 undoubtedly exhibits reduced, coordinatively unsaturated metal sites. Thus a redox HDS mechanism involving binding of thiophene to an electron-rich metal site, oxidative addition to the metal, sulfur removal, and reduction of the metal site is feasible. The calculated DOS for the (210) surface of RuS_2 suggests that the 4-coordinate Ru center could be easily reduced and could thus provide a site for oxidative addition and metal insertion into the thiophene ring, forming a surface complex whose structural and electronic properties are similar to those of **2**. Once again, however, this surface complex probably could not serve as a precursor for desulfurization, since desulfurization in the metal-inserted molecular complexes requires another coordination vacancy on the metal center. If the heterogeneous and homogeneous HDS reactions *can* indeed be related, the best

(21) Benson, J. W.; Angelici, R. J. *Organometallics* **1992**, *11*, 922.
(22) Harris, S. *Polyhedron* **1997**, *16*, 3219.
(23) Jones, W. D.; Dong, L. *J. Am. Chem. Soc.* **1991**, *113*, 559.
(24) Chen, J.; Daniels, L. M.; Angelici, R. J. *J. Am. Chem. Soc.* **1990**, *112*, 199.
(25) Bianchini, C.; Meli, A.; Peruzzini, M.; Vizza, F.; Moneti, S.; Herrera, V.; Sánchez-Delgado, R. A. *J. Am. Chem. Soc.* **1994**, *116*, 4370.
(26) Bianchini, C.; Meli, A.; Peruzzini, M.; Vizza, F.; Frediani, P.; Herrera, V.; Sánchez-Delgado, R. A. *J. Am. Chem. Soc.* **1993**, *115*, 2731.

candidate for an active site appears to be a 3-coordinate Ru center found on the RuS_2 (111) surface. Even in the stoichiometric (111) slab the surface Ru atoms are slightly reduced over the bulk Ru atoms, and the large stabilization of the surface Ru e_g band indicates that a 3-coordinate Ru surface atom should be easily reduced. Thiophene binding to a reduced metal followed by metal insertion into the ring still leaves one vacant coordination site; desulfurization could then proceed by a pathway analogous to the homogeneous reactions studied by Bianchini and others.

Conclusions

We have reported here the results of the first band structure calculations for Rh_2S_3. Although there is little experimental data for comparison, the calculated electronic structure is consistent with the features of the crystal structure of Rh_2S_3. The DOS reveals covalent σ bonding throughout the Rh−S network but only negligible Rh−S π bonding. The d^6 configuration of the Rh centers is responsible for the distorted octahedral coordination around each Rh center; an undistorted geometry would result in a net antibonding interaction between the Rh atoms in each face shared octahedral pair. The long Rh−Rh distances in these pairs makes such interactions impossible.

We have also carried out calculations on RuS_2. Comparisons of our results with both the experimental photoelectron spectrum and earlier ab initio calculations shows that the qualitative features of the band structure of RuS_2 are modeled quite well by our calculation. Although the crystal structure of RuS_2 is very different from that of Rh_2S_3, several similarities are observed in the electronic structures of the two materials. In particular, the four-coordinate tetrahedral geometry of the sulfur atoms in both sulfides appears to preclude metal−sulfur π bonding. Since the d^6 metals in both sulfides lie in an approximately octahedral environment, the lack of both metal−sulfur π interactions and metal−metal interactions leads to a narrow high energy occupied t_{2g} band which is localized on the Ru/Rh atoms. The absence of both metal−metal and metal−sulfur π interactions distinguishes both of these sulfides from MoS_2, another transition metal sulfide important in HDS catalysis. The nearly complete localization of electron density in the metal t_{2g} orbitals in these sulfides was also apparent in the results of earlier calculations on cluster models[27] and may play a role in their high HDS activity.

The results of calculations on the (210) and (111) surfaces of RuS_2 enable us to compare the electronic properties of 5-, 4-, and 3-coordinate surface Ru atoms. Stabilization of all or part of the Ru e_g band is observed for all three types of surface atoms; the stabilization increases with the degree of coordinative unsaturation. Comparisons can also be made between the electronic properties of the surface Ru atoms and the metal centers found in d^6 transition metal complexes that incorporate thiophenic ligands. These comparisons suggest that if the mechanisms for the heterogeneous HDS process occurring on RuS_2 and the homogeneous HDS reactions involving transition metal complexes are related, then the 3-coordinate Ru sites found on the (111) surface are the most likely candidates for active sites.

The calculations described here focused on the electronic properties of coordinatively unsaturated surface Ru atoms. Surface disulfides may also play a role in HDS catalysis, however, and future calculations will consider the role of the surface sulfurs in more detail.

Acknowledgment. Support of this work through National Science Foundation Grant CHE94-21784 is gratefully acknowledged. A.T. also thanks NSF EPSCoR for support.

IC971028N

(27) Harris, S.; Chianelli, R. R. *J. Catal.* **1984,** *86*, 400.